Physical and Numerical Simulation of Shear-Rate Dependent Viscosity in Polymer Flooding

Xin-gang Bu[1(✉)], Ming Han[2], Abdulkareem Alsofi[2], and Dong-qing Cao[1]

[1] Beijing Research Center, Aramco Asia, Beijing 100102, People's Republic of China
Xin.bu@aramcoasia.com
[2] EXPEC Advanced Research Center, Saudi Aramco, Dhahran 31311, Saudi Arabia

Abstract. High molecular polyacrylamides have been used widely in polymer flooding applications for improving oil production. The injected polymer is subjected to different shear rates and thus results in various performance. This paper integrates the behaviors of different laboratory experiments into a general workflow for evaluation of the impact of shear rate on oil production using numerical simulation. The impact of shear rates on the rheological property of a polymer solution was evaluated by injection of polymer solution into a core plug at different injection rates. The measured bulk viscosity and calculated apparent viscosity were fitted with different rheological models to identify flow behavior and the corresponding shear rate range. Shear rate at sand surface and shear rate profile from injector to deep formation were estimated using an inverted five-spot well pattern. Combination of the experimental results with the estimated shear rates was used to describe the flow behaviors of injected polymer solutions. The impact of shear-rate dependent viscosity on oil production was evaluated using a UTCHEM simulator. Laboratory experiments showed that polymer shear degradation occurs when the shear rate exceeds 4402 s^{-1} in a carbonate core plug with a permeability of 390 mD. The shear thickening was observed in the shear rate range of 90 to 4402 s^{-1}. The injected polymer solutions flowing from injector to near producer experience four viscosity regimes in sequence, i.e., shear degradation, shear thickening, shear thinning and Newtonian. The scales of each regime are different. The critical shear rates upon mechanical degradation are closely related to perforation parameters including perforation size, density, and interval. When the polymer solutions is injected into a reservoir with permeability of 390 mD at a rate of 0.2 pore volume/year, shear degradation occurs within a radius of 0.2 m around the wellbore, and shear thickening behavior between a radius of about 0.2 to 10 m, and the regimes of shear thinning or Newtonian flow in the rest range over a radius of 10 m to deep formation. The numerical simulation results show that polymer viscosity loss leads to oil production reduction, and shear thickening has very little effect on oil production if no considerable injectivity declines. The paper provides a workflow for evaluating the impact of shear rates on oil production from laboratory experiments to well scale polymer flooding by numerical simulation studies.

Keywords: Polymer flooding · Numerical simulation · Shear rate · Rheological property

J. Lin (Ed.): IFEDC 2021, SSGG, pp. 5273–5289, 2022.
https://doi.org/10.1007/978-981-19-2149-0_482

1 Introduction

Water-soluble polymers are wildly used in improved oil production through thickening the viscosity of injection water to reduce water permeability and improve the sweep efficiency. The application was defined as polymer flooding. Polyacrylamides (i.e., partially hydrolyzed polyacrylamide, HPAM) and biopolymers (i.e., xanthan gum) are the most common polymers applied in practice. Relative to biopolymers, the synthetic polymers such as HPAM is the most widely utilized due to its availability in large quantities with good viscosifying ability and low cost [1]. The viscosity of HPAM solutions is one critical parameter of rheological property, which has a significant effect on the performance of polymer flooding [2–5].

The injection rate is constant for most of polymer flooding performance evaluation with coreflooding experiment. This rate is low compared to the shear rate at which the shear degradation occurs reported by researchers [6–9, 18, 19]. Thereby, the impact of shear degradation on oil production is not reasonably evaluated. However, for the polymer flooding application in oilfields, the flow rate of injection polymer solutions varies over a wide range and changes dramatically near the injection well. Researchers [7, 20–22] reported that shear degradation to be greatest at the entry plane of the injection sand face. Similar conclusions also presented that the polymer viscosity loss occurs in the vicinity of an injection well because of shear degradation [13, 14, 18, 23, 24]. Dupas et al. [18] concluded that extensional viscosity decreased more than the shear viscosity, which resulted in much less resistance in porous media even at no shear viscosity loss. This conclusion was also drawn by other researchers [6, 10, 13, 14].

The injection rate is constant for most of polymer flooding performance evaluation with coreflooding experiment. This rate is low compared to the shear rate at which the shear degradation occurs reported by researchers [6, 16–19]. Thereby, the impact of shear degradation on oil production is not reasonably evaluated. However, for the polymer flooding application in oilfields, the flow rate of injection polymer solutions varies over a wide range and changes dramatically near the injection well. Researchers [7, 20–22] reported that shear degradation to be greatest at the entry plane of the injection sand face. Similar conclusions also presented that the polymer viscosity loss occurs in the vicinity of an injection well because of shear degradation [13, 14, 18, 23, 24]. Dupas et al. [18] concluded that extensional viscosity decreased more than the shear viscosity, which resulted in much less resistance in porous media even at no shear viscosity loss. This conclusion also were presented by [6, 10, 13–15].

In this study, we investigate the shear rate at which shear degradation occurs and viscosity loss by coreflooding test. The bulk viscosity and apparent viscosity are fitted with three different models for identifying the shear rate range of different flow behavior. We calculate the flow rate and the corresponding shear rate of polymer solution flowing from injection well to near producer for an inverted 5-spot well pattern based on general assumptions. Combining the results of experimental and calculations, we use numerical simulation methods to bridge the gap between laboratory and oilfield for evaluating the impact of shear rates on the performance of polymer flooding application in oilfields.

2 Shear Degradation Tests

In previous work [19], the polymer solutions were injected into core plugs at step increasing flow rate to evaluate the effect of shear degradation on bulk viscosity and apparent viscosity. The polymer used in the experiments is a sulfonated polyacrylamide with a molecular weight of 14 million g/mol and hydrolysis degree of 4.2%. Two carbonate core plugs with significant difference in permeability were used in the experiments, the detailed information were given in Table 1. The previous experimental data and results are used for this work. The experimental results show that for the core plug with a permeability of 390 md, the viscosity loss occurred when the injection rate exceeds 20 ml/min. For the other core plug with a permeability of 60 md, the viscosity loss was found when the injection rates above 2 ml/min. The bulk viscosities of the sheared samples at different injection rates in the core shear degradation experiments were shown in Figs. 1, 2 and 3 shows the viscosity loss of the polymer solutions after flow through the carbonate core C31 and C59.

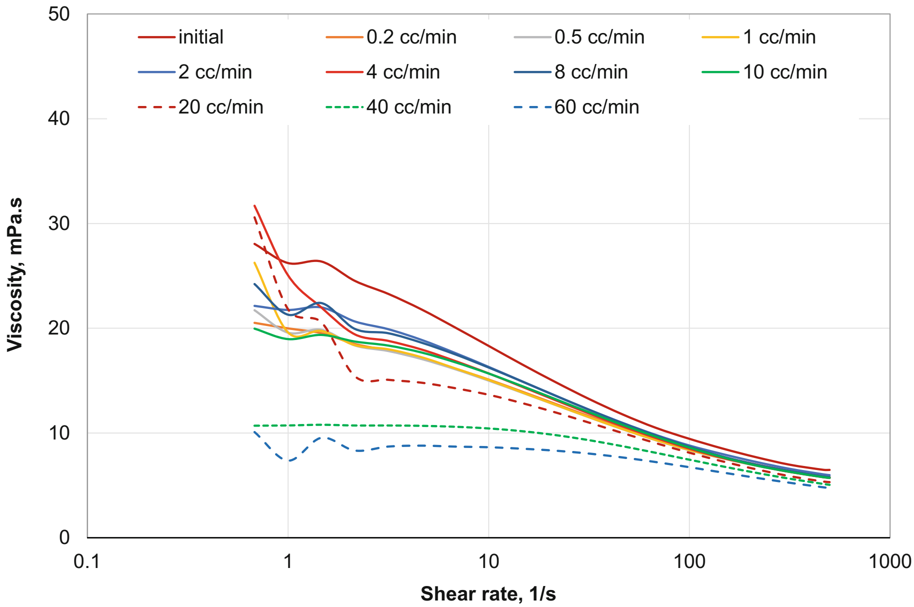

Fig. 1. Viscosity of produced polymer versus shear rate, C31 core plug

Table 1. Core plug information in the shear degradation tests

Core No	Length, cm	Diameter, cm	Porosity, %	Brine Perm, mD
C31	4.15	3.82	26.18	390
C59	4.92	3.81	22.48	60

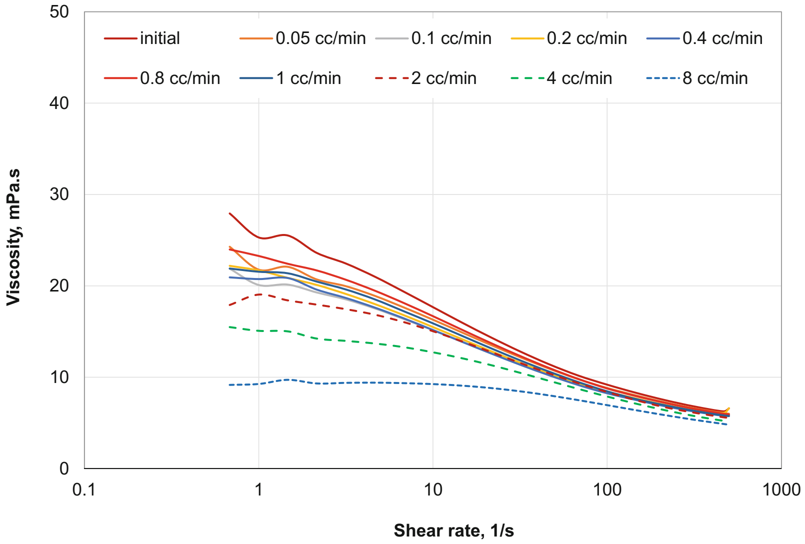

Fig. 2. Viscosity of produced polymer versus shear rate, C59 core plug

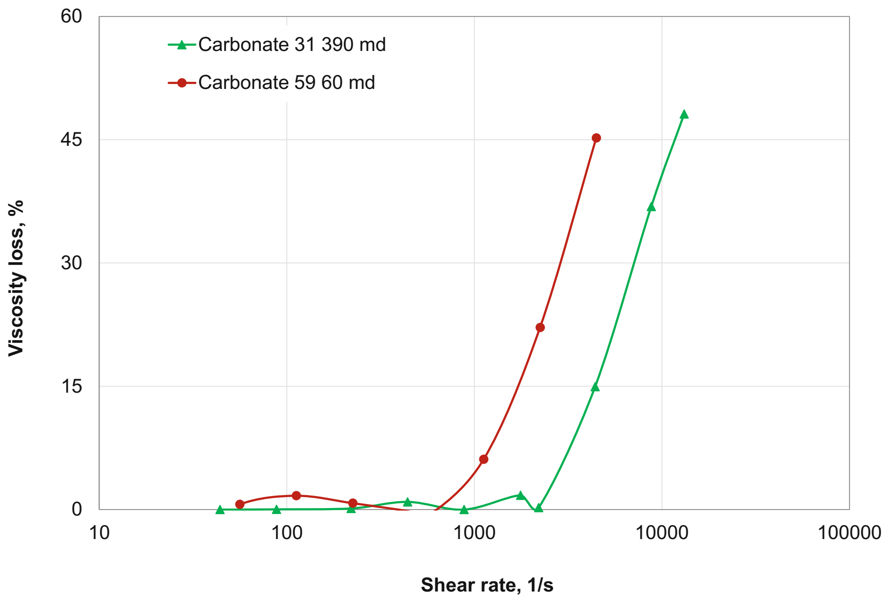

Fig. 3. Polymer viscosity loss in shear degradation tests

3 Modeling of Viscosity

In this study, there are two kinds of viscosity involved. One is the viscosity measured with Rheometer in the laboratory as bulk viscosity. The other is the viscosity calculated from the experimental data of coreflooding using Darcy's law as apparent viscosity. These two kinds of viscosity can be seen everywhere in published papers. Here, we refer to these viscosity values only to indicate its data source.

3.1 Shear Rate

Shear rate was defined as the rate of change of velocity at which one layer of fluid passes over an adjacent layer. It can be considered as a gradient velocity and depends on flow velocity and radius of tube/vessel. Testing data of Rheometer shows that the viscosity is a function of shear rate. However, for the coreflooding experiments and pilot tests, injection rate is a commonly used parameter. Thereby, we need to correlate injection rate with shear rate to evaluate the effect of injection rate on the viscosity of polymer solutions. Different correlation equations were proposed in published papers related to rheology of HPAM solutions [11, 25, 26]. These equations with similar format but impact factors were considered differently. Equation 1 is one equation widely used to convert flow rate into shear rate, and also is similar to the model used in UTCHEM simulator [11].

$$\gamma_{\text{eff}} = \mathrm{C}\left[\frac{3\mathrm{n}+1}{4\mathrm{n}}\right]^{\frac{\mathrm{n}}{\mathrm{n}-1}} \frac{\mathrm{u}}{\sqrt{\mathrm{k}\mathrm{k}_{\mathrm{rw}}\mathrm{S}_{\mathrm{w}}\text{Ø}}} \quad (1)$$

where u is Darcy velocity of the polymer solutions; k is the average permeability in m^2; k_{rw} is the water relative permeability; S_w is water saturation; Ø is porosity; n is the "power-law" index. C is a factor related to permeability and porosity. Cannella et al. [25] reported that Eq. (1) fits a variety of core flooding data well when C equal to 6.

3.2 Carreau Model for Bulk Viscosity

A widely employed rheological model is Carreau model for describing shear-thinning behavior of polymers [25]. It can describe the viscometer-measured viscosity over the entire range of shear rates including a low shear rate Newtonian region, a shear-thinning "power-law" region, and a high shear rate Newtonian plateau.

$$\mu = \mu_\infty + \left(\mu_p^0 - \mu_\infty\right)\left[1 + (\lambda_1\gamma_{\text{eff}})^a\right]^{(n_1-1)/a} \quad (2)$$

where μ is the steady-shear bulk viscosity, μ_p^0 and μ_∞ are the limiting Newtonian viscosities at the low and high shear limits, respectively; γ_{eff} is the effective shear rate; n_1 is the "power-law" index; λ_1 is a time constant representing the relaxation time; It can be determined as the inverse of the shear rate associated with the intersection of two straight lines fitted through the experimental data for the lower Newtonian and shear thinning regimes; and a is generally taken to be 2.

3.3 Rheological Models for Polymer Solution in Porous Media

Unified viscosity model. Delshad et al. [11] presented an apparent viscosity model that can be applied to the full spectrum of Newtonian, shear-thinning and shear-thickening regimes. In this model, via the effective shear rate, the apparent viscosity can be correlated with Darcy velocity. The model was developed based on the premise that the apparent viscosity of the polymer solution is a sum of the shear dominating viscosity and the elongational-dominating viscosity:

$$\mu_{app} = \mu_{\infty} + \left(\mu_p^0 - \mu_{\infty}\right)\left[1 + (\lambda_1 \gamma_{\text{eff}})^a\right]^{\frac{n_1 - 1}{a}} + \mu_{\max}\left[1 - \exp\left(-(\lambda_2 \tau_r \gamma_{\text{eff}})^{n_2 - 1}\right)\right] \tag{3}$$

where μ_{app} is the apparent viscosity in porous media; τ_r is the characteristic relaxation time; $\mu_{\max}$ is a plateau value of viscosity beyond which shear degradation will occur, λ_2 and n_2 are empirical constants, the meaning of other parameters are same as Carreau model.

Stavland Model. Stavland et al. [12] measured the effluent viscosity and found that the viscosity loss occurs while the shear rates exceed a critical value associated with the onset of degradation. They proposed a model that can describe shear degradation, also with function of shear thinning and shear thickening.

$$\mu_{app} = \mu_{\infty} + \left[\left(\mu_p^0 - \mu_{\infty}\right)\left((1 + \lambda_1 \gamma_{\text{eff}})^{\text{n}_1} + \left(\lambda_2' \gamma_{\text{eff}}\right)^m\right)\right] \cdot \left[1 + (\lambda_3 \gamma_{\text{eff}})^x\right]^{j/x} \tag{4}$$

where m is a non-zero tuning parameter known as the elongation exponent, the onset of elongation given by λ_2', $1/\lambda_3$ represents the onset of shear degradation, can be determined by analyzing the viscosity of core flood effluent, j is a shear thinning exponent of experimentally matched and x is a tuning parameter.

3.4 Application of Rheological Models

The rheological models described previously were employed to fit the data from experiments conducted by Dongqing et al. [19]. The experimental data and fitting curves are presented in Fig. 4, and the parameters used for all models are listed in Table 2. The hollow points in blue circles represent the bulk viscosity of a polymer solution with concentration of 2000 ppm, which is prepared using sulfonated polyacrylamide with a molecular weight of 14 million g/mol and hydrolysis degree of 4.2%. The solid points represent the apparent viscosity calculated from the experimental data of core flooding.

Figure 4 shows the results of experimental data fitted with Carreau model, UVM and Stavland models. The bulk viscosity measured using rheometer were well fitted with Carreau model as shown in red line, which indicates a typical shear thinning characteristic of polymer solutions. The apparent viscosities deviate significantly from bulk viscosity due to the shear-thickening behavior of the polymer solution flowing in porous media, which caused by the elongation of the molecular above a certain shear rate. The apparent viscosity in green and blue colors are calculated from experiments with core plug permeability of 60 and 390 mD, and the corresponding shear thickening rate ranges are 10–1122 and 20–4402 1/s, respectively. This difference is probably due to the different properties of the two carbonate core plugs and the calculation method, because both experiments were conducted with the same polymer. The apparent viscosity first increased and then decreased with the shear rate, and was well matched using Stavland model. But for the UVM model, the apparent viscosity above the shear degradation rate is not fitted. Because the author posed a maximum apparent viscosity at shear degradation rate while the apparent viscosity reach it and then keep constant with shear rate increase, and the shear degradation is not simulated in the model. The Stavland model well simulated all flow behavior of polymer solutions in porous media. The fitted curve of Stavland model indicates the flowing behavior of polymer solution in porous media. Take the experimental data C31 fitted by Stavland model as an example. The polymer solution shows shear thinning behavior when the shear rate is lower than 20 1/s. When the shear rate is greater than 3000 1/s (estimated from the fitted curve in blue dotted line), the polymer solution is shear degraded. When the shear rate is in the range of 20–3000 1/s, the polymer exhibits shear thickening behavior.

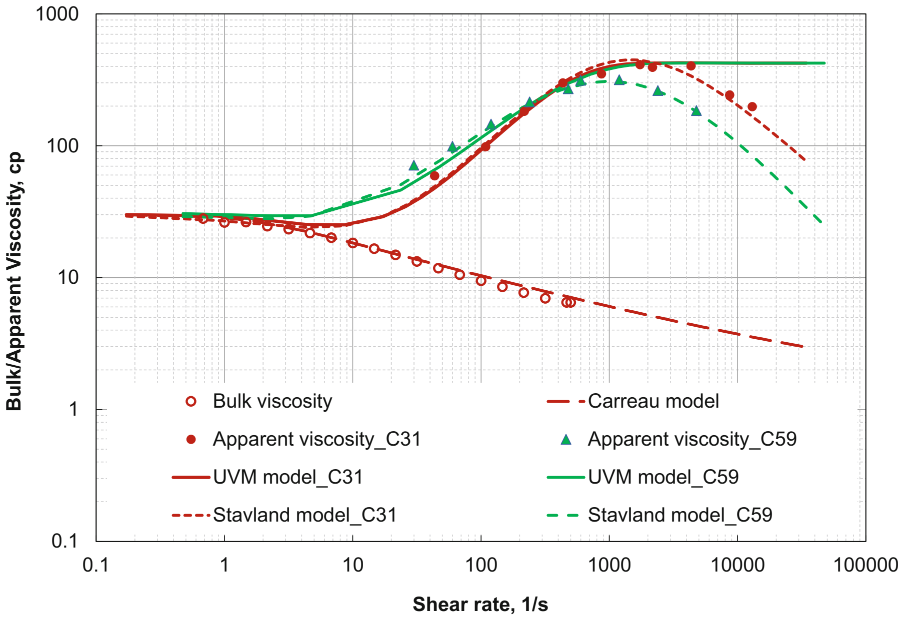

Fig. 4. Comparison of different models fit for polymer used in experiments

Table 2. Fitting parameter for 3 viscosity models

Parameter	Carreau model	Unified viscosity model	Stavland model
μ_{∞},cp	1.05		
$\mu_0{}^p$,cp	30		
n_1	0.73		
n_2	–	2.1	
λ_1, S	0.67		
λ_2, S		0.03	
τ_r, S	–	0.083	–
μ_{max},cp	–	420	–
λ'_2, S	–	–	0.03
λ_3, S	–	–	0.0008
m	–	–	1.1
x	–	–	1.1
j	–	–	−2

4 Impact of Shear Rate Dependent Viscosity on Polymer Flooding

4.1 Well Pattern and Polymer Solution

Inverted five-spot well pattern is a popular style and widely employed in chemical flood projects, which is one central injector surrounding with four producers [27, 28]. In this work, inverted five-spot well pattern was selected for the study aim to achieve general results, and the well space is 250 m, which is the distance between the injector and producer.

The interested polymer is sulfonated polyacrylamide with a molecular weight of 14 million g/mol and hydrolysis degree of 4.2%. The polymer solution is 2000 ppm prepared with high salinity brine containing 57,670 mg/L total dissolved solids.

4.2 Well Completion Mode

Completion model of injection wells has much effect on the performance of polymer flooding. Because the flux area is closely related to completion model, which is a key parameter for determining the flux. In this work, we focus on the completion model of casing perforation. Casing perforation is a typical way for chemical injection wells. It help to achieve selective perforating oil reservoir with different pressure and physical properties in order to avoid interlayer interference, and keep clear of interbedded water and bottom water. And provide the conditions of separate-zone operations, including separate-zone injection and production and selective fracturing and acidizing [28]. For a perforated casing completion injection well, the flow rate of injected fluids behind the perforation is closely related to perforation intervals, shot density and estimated perforation length, because all of these have effect on flow area and flow behavior. The parameter of perforation surface area used in this study is an average value, which is calculated from the data collected by Smith [29]. The penetration depth is calculated based on the perforation surface area and the diameter.

4.3 Estimation of Shear Rate

The viscosity of HPAM solution is a shear rate dependent property. The shear rate is estimated from flow rate using the models described previous, which is affected by many factors including reservoir permeability, flux area, resistance factor of polymer et al. During the polymer solutions flow from wellbore to deeper reservoir formation, the flow rate away from wellbore is easier to calculate in comparison with that around wellbore. Because the flow behavior is more complicated around wellbore for the casing perforation wells. To better estimate the magnitude and change of shear rate, we first calculate the flow rate of the polymer solution passing through the perforations, and the corresponding shear rate. Then to estimate the flow rate from injector to near producer and the matching shear rate. The reservoir properties and perforation information used for the calculation were listed in the Table 3. For the purpose of simplification of calculation procedure the below assumptions were made.

- The injector is a casing perforation completion well;
- Oil saturation is residual oil saturation to get a maximum water saturation around wellbore;
- The relative permeability of water phase is 1 to get a minimum shear rate;
- The flux of pass through each perforation is equal;
- The flow rate at the point where hemispherical flow transition to radial flow is equal;

Table 3. Parameters for calculation of flux

Well pattern	Inverted 5-spot	Shot density, /m	12
Well space, m	250	Perforation diameter, m	0.0107
Permeability, mD	390	Penetration depth, m	0.35
Porosity, fraction	0.23	Perforation surface area, m^2	0.0134
Injection Rate, Pv/a	0.2		

Table 4. Parameters for flow rate estimation

PV/m, m^3	Injection Rate, Pv/a	q/perforation, m^3/day	Flux, pass through perforation, m/s	Flux, at perforation surface, m/s
28750	0.2	1.452	0.214	0.00125

Shear rate in perforation and at perforation surface. The polymer solution first flow through the perforation and then the perforation surface during polymer injection. Based on the assumptions made previously and parameters listed in the Table 4, we using the Eq. (5) to calculate the shear rate which is applicable for calculating shear rate for polymer solutions entering perforations or fractures [29].

$$\gamma = \frac{8\mu}{d} \tag{5}$$

where μ is the fluid flux, or linear velocity in m/s, through an orifice of diameter d, m.

According to Eq. (5), polymer solutions will experience a shear rate of about 171 1/s when passing through the perforation for the given conditions as listed in Table 3. After passing through the perforation, the polymer solution reaches the perforation surface and then starts to flow into the porous medium. A simple method as Eq. (6) from published paper [29] was used to estimate the shear rate at perforation surface.

$$\gamma = \frac{2\mathrm{u}}{\sqrt{2\mathrm{k}_p S_w \emptyset}} \tag{6}$$

where u is Darcy velocity of the polymer-containing water phase; k_p is calculated by dividing the permeability of the core to brine, k_b, by the polymer apparent viscosity in the porous media, μ_{app}; S_w is water saturation; Ø is porosity. The flux at perforation surface is calculated by dividing the flow rate by the perforation surface area. If it is assumed that the polymer viscosity changes between 6.5–25 cp of the bulk viscosity before entering the perforation surface, the estimated shear rate using Eq. (6) is 15198–29806 1/s, which far exceeds the critical shear degradation rate of 4402 1/s obtained from the experiments. This means that the shear degradation of the polymer solutions occur at the moment of entering the reservoir formation from the perforation surface. If the apparent viscosity at the moment of entering the perforation surface is higher than the bulk viscosity, the shear rate will be higher and the shear degradation is more severe.

Shear Rate Profile. The basic knowledge that the pressure drop changes dramatically around wellbore, thereby changes in flow rate and the corresponding shear rate. For a perforated casing completion injection well, the flow behavior around wellbore is more complicated. Mcleod [30] assumed that the actual three-dimensional flow pattern could be approximated by pure radial flow to the perforation tips followed by local radial vertical flow convergence into individual tunnels. Amer [31] further developed this idea and show that the flow distribution is characterized by concentration at the tip of the perforation with an approximately hemispherical flow. Based on these research results we assume that the flow direction of injection well is opposite to that of producer but the flow behavior is similar, that is hemispherical flow occurs around perforation followed by pure radial flow to deeper formation. The local flow distribution is illustrated diagrammatically in Fig. 5.

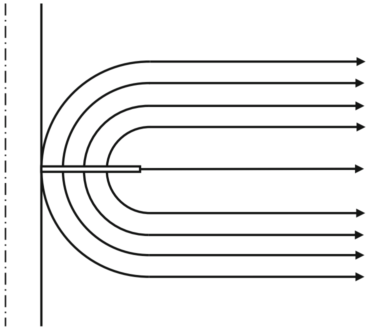

Fig. 5. Hemispherical flow and radial flow around perforation

Figure 6 shows the profiles of estimated Darcy velocity and the corresponding shear rate from injector to near producer. It can be seen that the flow rate changes dramatically in the vicinity of wellbore over a narrow range due to the impact of perforation and flow area variation, out of this range all flow is radial or laminar flow based on the assumptions. The flow rates exceed 10 m/day around wellbore within a radius of 0.2 m, which is great than the rates that can induce shear degradation reported by researchers [6, 19]. After the polymer solution flow from wellbore over 3 m, the flow rates reduced to 1 m/day for the study case.

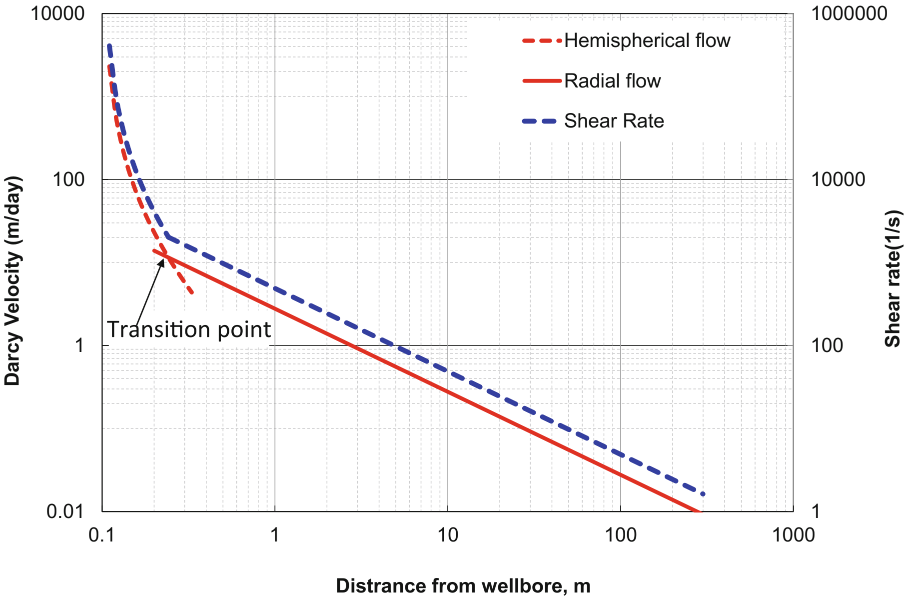

Fig. 6. Profiles of Darcy velocity and shear rate from injector to producer

4.4 Viscosity Regimes

Polymer viscosities, including bulk viscosity and apparent viscosity, are sensitive to shear rate. Based on the estimated profile of shear rate from injector to producer, viscosity profiles of the injected polymer were estimated with UVM and Stavland model as show in Fig. 7. It can be seen that there is significant difference in the apparent viscosity predicted using UVM and Stavland models within a radius of about 0.2 m from wellbore. This difference is caused by the model itself, because the UVM model cannot simulate polymer shear degradation. The change in apparent viscosity predicted with Stavland model indicates that the injected polymer solutions will experience four different flow regimes, which are shear degradation, shear thickening and shear thinning or non-Newtonian from the wellbore of injector to deeper reservoir formation. For the specific reservoir properties and the interesting polymer of this study, the range of shear degradation is in a radius of 0.2 m from wellbore, the range of shear thickening is in a radius of 0.2 to 20 m, and the range of shear thinning or non-Newtonian is in a radius over 20 m.

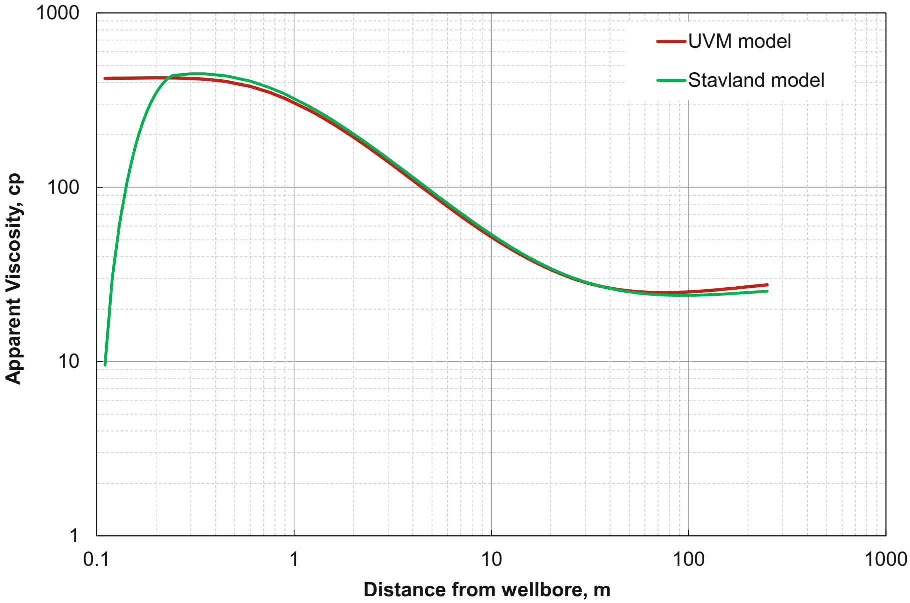

Fig. 7. Predicted viscosity profiles with different models

4.5 Impact of Shear Rate Dependent Viscosity on Polymer Flooding

When a polymer solution of HPAM is injecting into a well which without fractures around wellbore, the greatest shear (mechanical) degradation resulting from highest flow rate will occur in a small range around wellbore, then the flow rate will decrease as the solutions penetrates deeper into the formation, which means no further significant mechanical degradation of the polymer will occur [4, 17]. In this study, we assumed that the injected polymer is a pre-sheared polymer and ignore the process of shear degradation. Because the range in which shear degradation occurs is very small relative to the well space between injector and producer, and the apparent viscosity in this range cannot be simulated accurately because the gridblock size of the geological model generally is great than the range of shear degradation. But the viscosity loss and resistance factor reduction resulting from shear degradation are obvious and should be considered for prediction the performance of polymer flooding.

Numerical simulation method was used to investigate the impact of shear rate dependent viscosity on oil recovery. A 2-dimensional heterogeneous model was built for this study. The properties of the model is listed in Table 5. UTCHEM simulator 2012 was used since which is good simulator for simulation of chemical flooding. The simulator with the function of shear thickening, but without accounting for the shear degradation [6]. Five cases were designed to investigate the effect of shear rate change on polymer flooding, and the details of cases are given in Table 6. The value of viscosity loss is assumed according to practical experience and reports. Case 1 is the simplest case because only shear thinning was considered, and the result is used as a basis for comparison with other cases. Case 2 is taken the function of shear thickening into account on the basis of case 1. For the shear degradation simulation cases 3 to 5, we assumed the injecting polymer as pre-sheared polymer which is the output polymer experienced shear degradation, and the assumption is a simple way to take shear degradation into account based on the reason described previously.

Table 5. 2-D simulation model properties

Number of grid-block	113 × 113 × 1
Model size, m	250 × 250 × 1
Porosity, fraction	0.23
Brine Permeability, mD	390
Initial water saturation, fraction	0.65
Injection Rate, Pv/a	0.2
Polymer concentration, wt. %	0.2

Table 6. Details of simulation cases

No.	Rheological properties were modeled
Case 1	Only shear thinning
Case 2	Shear thinning and shear thickening
Case 3	Shear thinning and shear thickening, shear degradation is simulated via pre-sheared polymer, viscosity loss of 15%, resistance factor loss of 15%
Case 4	Shear thinning and shear thickening, shear degradation is simulated via pre-sheared polymer, loss of 15%, resistance factor loss of 25%
Case 5	Shear thinning and shear thickening, shear degradation is simulated via pre-sheared polymer, loss of 25% and resistance factor loss of 44%

The simulated oil production and average pressure of cases are shown in Fig. 8 and 9, it can be found that the oil production of case 1 and 2 are almost the same, which indicated that the effect of shear thickening on oil production is very limited. The reason for this result is that the shear thickening just occurs in small space, and in a larger space where polymer solutions show the behavior of shear thinning. The results of cases 3 to 5 shows that oil production decrease with the loss of resistance factor increase due to declined capacity of mobility control. For case 3 and case 4, the injected polymer solutions with same viscosity but different resistance factor, it can be seen that oil production declined as more resistance factor loss. Also the shear degradation cases illustrated that the loss degree of resistance factor is critical and should be evaluated during polymer screening. The impact of shear degradation on the average pressure of reservoir is similar to the oil production if the changes in injectivity is ignored. In polymer flooding, the injectivity is affected by many factors such as resistance factor of polymer solution, fracturing pressure of reservoir and injection rate. In practice, polymer injection generally causes the injectivity to decrease, thereby, the decreased injection rate in comparison to water injection. This make the change in oil production and average pressure is more complicated, but the trend of the impact on that will not change.

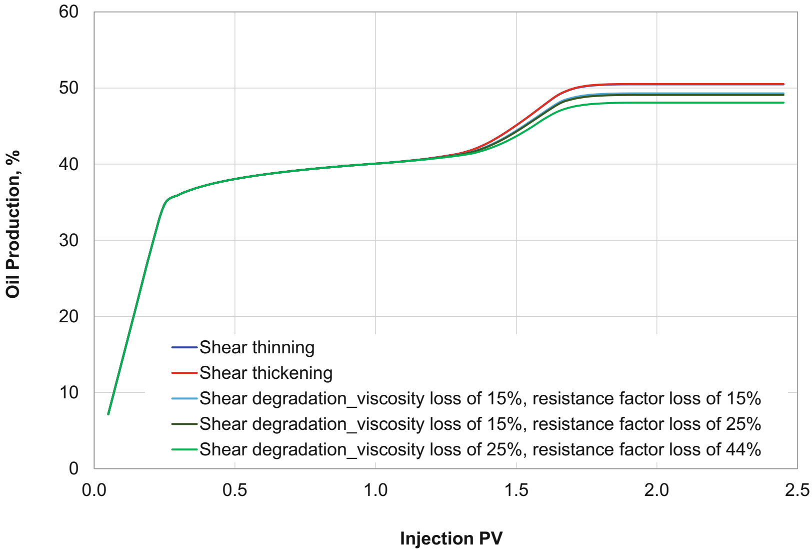

Fig. 8. Effect of shear degradation on oil production

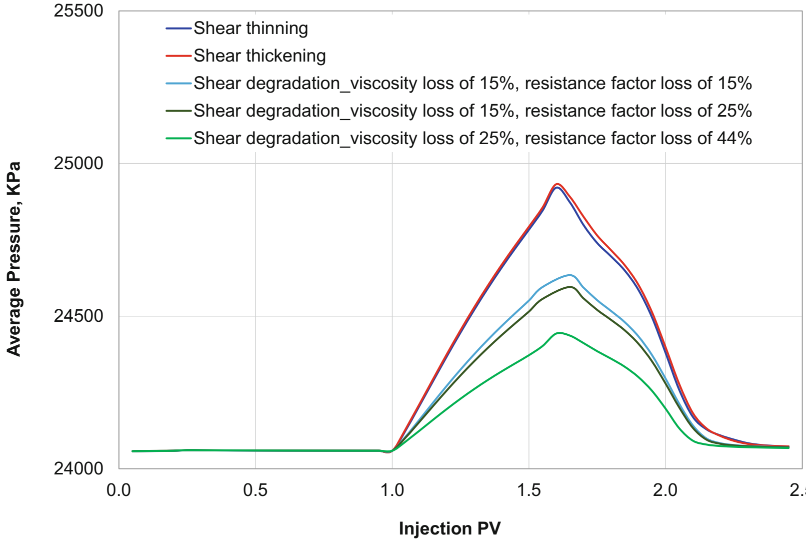

Fig. 9. Effect of shear degradation on average pressure of reservoir

5 Conclusions

- The shear rates that the polymer solution suffers from the injector to the producer varies in a widely range of about 5–100000 1/s.
- The injected polymer solutions experience four viscosity regimes that are shear degradation, shear thickening and shear thinning or non-Newtonian.
- When the polymer is injected into a 390 mD reservoir at a rate of 0.2 pore volume/year, shear degradation occurs within a 0.2 m radius around the wellbore, and shear thickening occurs within a radius of about 0.2 to 10 m.
- Shear thickening has very limited impact on oil production since the shear thickening occurred in a very small area in vicinity of well location.
- Shear degradation has a significant impact on polymer flooding to make the decrease in oil production and average pressure of reservoir.

References

1. Wang, D., Han, P., Shao, Z., Chen, J., Seright, R.S.: Sweep improvement options for the Daqing oil field. In: Paper SPE 99441 Presented at SPE/DOE Symposium on Improved Oil Recovery, Tulsa, OK, USA (2006)
2. Kim, D.H., Lee, S.J., Ahn, C.H., Huh, C., Pope, G.A.: Development of a viscoelastic property database for EOR polymers. In: Paper SPE 129971 Presented at Improved Oil Recovery Symposium, Tulsa, Oklahoma, USA (2010)
3. Sochi, T.: Non-Newtonian flow in porous media. Polymer **51**, 5007–5023 (2010)
4. Seright, R.S.:"The effects of mechanical degradation and viscoelastic behavior on injectivity of polyacrylamide solutions. SPE J. **23**, 475–485. SPE 9297 (1983)

5. Heemskerk, J., Jansen-Van, R., Rosmalen, R., Holtslag, R.J., Teew, D.: Quantification of viscoelastic effects of polyacrylamide solutions. In: Paper SPE 12652 Presented at SPE/DOE Fourth Symposium on EOR,15–18 April, Tulsa, OK (1984)
6. Stavland, A., Jonsbraten, H., Lohne, A., Moen, A., Giske, N.H.: Polymer flooding - flow properties in porous media versus rheological parameters. In: Paper SPE 131103 Presented at the SPE EUROPEC/EAGE Annual Conference and Exhibition, 14–17 June, Barcelona, Spain (2010)
7. Seright, R.S., Seheult, J.M., Talashek, T.: Injectivity characteristics of EOR polymers. In: Paper SPE 115142 Presented At SPE Annual Technical Conference and Exhibition, 21–24 September, Denver, Colorado, USA (2008)
8. Sorbie, K.S.: Polymer Improved Oil Recovery. Blackie, Glasgow-London (1991)
9. Zaitoun A., Makakou P., Poweletc N.B.: Shear stability of EOR polymers. In: Paper SPE 141113 Presented at the SPE International Symposium on Oilfield Chemistry held in The Woodlands, Texas, USA (2011)
10. Jennings, R.R., Rogers, J.H., West, T.J.: Factors influencing mobility control by polymer solutions. J. Pet. Tech. **23**(3), 391–50. SPE 2867-PA (1971)
11. Hirasaki, G.J., Pope, G.A.: Analysis of factors influencing mobility and adsorption in the flow of polymer solution through porous media. SPE J. **14**(4), 337–346. SPE-4026-PA (1974)
12. Masuda, Y., Tang. K.-C., Mlyazawa, M., Tanaka, S.: 1D simulation of polymer flooding including the viscoelastic effect of polymer solution. SPE Res. Eng. **7**(2), 247–252. SPE 19499-PA (1992)
13. Maerker, J.M.: Shear degradation of partially hydrolyzed polyacrylamide solutions. SPE J. **15**(4), 311–322, Trans., AIME, 259. SPE 5101-PA (1975)
14. Southwick J.G., Manke C.W.: Molecular degradation, injectivity, and elastic properties of polymer solutions. In: Paper SPE 15652 Presented at the SPE Annual Technical Conference and exhibition held In New Orleans, Oct. 5–8 (1986)
15. Ghoniem, S., Chauveteau, G., Moan, M., Wolff, C.: Mechanical degradation of semi-dilute polymer solutions in laminar flows. Can. J. Chem. Eng. **59**, 450–454 (1981)
16. Ghoniem, S.A.A.: Effect of deformation sequence on rheological behavior and mechanical degradation of polymer solutions. Chem. Eng. Commun. **63**, 129 (1988)
17. Seright, R.S., Maerker, J.M., Holzwarth, G.: Mechanical degradation of polyacrylamides induced by flow through porous media. Am. Chem. Soc. Polym. Prepr. **22**(August), 30–33 (1981)
18. Argillier, J.F., et al.: Impact of polymer mechanical degradation on shear and extensional viscosities: toward better injectivity forecasts in polymer flooding operations. In: SPE 164083 Presented at International Symposium on Oilfield Chemistry, 8–10 April, The Woodlands, Texas, USA (2013)
19. Cao, D., Han, M., Leng, Z., Wang, J.: Laboratory study on polymer mechanical degradation in carbonate core plugs versus in capillary tubes. In: Paper Presented at the SPE Kuwait Oil and Gas Show and Conference, Mishref, Kuwait, October (2019)
20. Wang, D.M., Cheng, J.C., Wu, J.Z., Wang, G.: Experiences learned after production more than 300 million barrels of oil by polymer. In: Paper SPE 77693 Presented at Annual Technical Conference and Exhibition, San Antonio, Texas, on 29 September (2002)
21. Littmann, W., Kleinitz, W., Christensen, B.E., Stokke, B.T., Haugvallstad, T.: Late results of a polymer pilot test: performance, simulation adsorption, and xanthan stability in the reservoir. In: Paper 24120-MS Presented at the SPE/DOE Enhanced Oil Recovery Symposium, Tulsa, Oklahoma, 22–24 April (1992)
22. Puls, C., Clemens, T., Sledz, C., Kadnar, R., Gumpenberger, T.: Mechanical degradation of polymers during injection, reservoir propagation and production - field test results 8 TH reservoir, Austria. In: Paper SPE-180144 Presented at the SPE Europec Featured at 78th EAGE Conference and Exhibition, Vienna, Austria (2016)

23. Warner Jr., H.R.: Analysis of mechanical degradation data on partially hydrolyzed polyacrylamide solutions. SPE-6502-MS (1976)
24. Martin, F.D.: Mechanical degradation of polyacrylamide solutions in core plugs from several carbonate reservoirs. SPE J. **1**, 139–148. SPE 12651-PA (1986)
25. Canella, W.J., Huh, C., Cohen, R.E.: Prediction of xanthan rheology in porous media. In: Paper SPE 18089, Presented at SPE Annual Tech. Conf., Houston, TX (1988)
26. Chauveteau G., Denys K., Zaitoun A.: New Insight on polymer adsorption under high flow rates. In: Paper SPE 75183 Presented at SPE/DOE Improved Oil Recovery Symposium, 13–17 April, Tulsa, Oklahoma (2002)
27. Pu, H., Xu, Q.: An update and perspective on field-scale chemical floods in Daqing oilfield, China. In: Paper SPE 118746 presented at SPE Middle East Oil and Gas Show and Conference held in the Bahrain International Exhibition Center, Kingdom of Bahrain (2009)
28. Renpu, W.: Advanced Well Completion Engineering, Third Edition. Gulf Professional Publishing (2011)
29. Smith, J.E.: Closing the lab-field gap: A look at near-wellbore flow regimes and performance of 57 field projects. In: Paper SPE-27774 Presented at SPE/DOE Ninth Symposium on Improved Oil Recovery Held in Tulsa, Oklahoma (1994)
30. Mcleod, H.O.: The effect of perforating conditions on well performance. In: Paper SPE 10649 Presented at the 1982 SPE Formation Damage Control Symposium Held in Lafayette, LA (1983)
31. Amer M.S., Stewart, G.: New approach towards understanding of near well bore behavior of perforated completions. In: Paper SPE 36866 Presented at the SPE European Petroleum Conference Held in Milan, Italy (1996)